OPTIMIZATION OF FORGING PROCESSES WITH A CONCURRENT APPROACH

by

Murat Öztürk

B.S., in Mechanical Engineering, Bogazici University, 2005

Submitted to the Institute for Graduate Studies in
Science and Engineering in partial fulfillment of
the requirements for the degree of
Master of Science

Graduate Program in Mechanical Engineering
Boğaziçi University
2009

ACKNOWLEDGEMENTS

I would like to thank my advisor Assoc. Prof. Fazıl Önder Sönmez for his guidance, patience and continuous support during the preparation of this thesis.

I would like to express my gratitude to the assistants and colleagues at the Department of the Mechanical Engineereing of Boğaziçi University, especially Ahmet H. Ertaş, Niyazi Tanlak and Haluk Tümer, for their support and motivation. Finally, I would like to thank my family for their support, patience and encouragements.

The Scientific and Technological Research Council of Turkey (TUBITAK) is gratefully acknowledged for supporting this thesis.

This thesis work was supported by the Scientific Research Projects of Bogazici University with the code number 08A602.

ABSTRACT

OPTIMIZATION OF FORGING PROCESSES WITH A CONCURRENT APPROACH

With the increasing complexity of manufacturing processes and the interrelations between the different phases, the possibility of a phase being affected by a preselected design variable is very high. In that case, the influence of a design variable not only on the part performance of but also on the feasibility and efficiency of its manufacturing should be considered. Concurrent engineering approaches should then be adopted to take the control of such complicated relations among the subprocesses.

In this thesis, a concurrent design optimization methodology was proposed to minimize the cost of a cold forged manufacturing process using the design parameters as optimization variables. An objective function was defined combining material cost, manufacturing cost, and post manufacturing (shearing) cost of the product. The part to be optimized was a simply supported I-beam under centric load. Nelder-Mead was selected as the search algorithm and analysis was carried out using commercial finite element software, ANSYS.

Some geometric parameters were chosen as optimization variables: the rib radiuses, die land, and burr thickness. After finding the optimum values for these parameters within the feasible domain, some design guidelines were proposed. The most effective parameter on the overall cost was found to be the die land and the most dominant term among the three cost terms was found to be the material cost.

ÖZET

EŞZAMANLI YAKLAŞIM İLE DÖVME İŞLEMİ OPTİMİZASYONU

Çok safhalı üretim süreçlerindeki karmaşıklık ve safhalar arası ilişkiler arttıkça, ileri bir safhalardaki ilk aşamalarda belirlenen bir değişkenden etkilenme ihtimali artıyor. Alt safhalardaki böylesi karmaşık ilişkileri kontrol edebilme noktasında eşzamanlı mühendislik yaklaşımları büyük önem taşımaktadır.

Bu tez çalışmasında, soğuk dövme ile üretilen bir parçanın malzeme maliyeti dizaynından üretim sonrası operasyonlarına kadar olan süreçteki toplam maliyetini minimize edecek bir eşzamanlı dizayn optimizasyonu metodu önerilmiştir. Minimize edilecek hedef fonksiyonu içinde malzeme maliyeti, üretim maliyeti ve üretim sonrası operasyon(çapak kesme) maliyetini içinde barındıracak şekilde tanımlanmıştır. Optimize edilecek parça merkezden yüklenmiş basit mesnetli bir I-profildir. Arama algoritması olarak Nelder-Mead metodu seçilmiş ve analiz ANSYS sonulu elemanlar programı kullanılarak yapılmıştır.

TABLE OF CONTENTS

LIST OF FIGURES

LIST OF TABLES

LIST OF SYMBOLS

A	Projected area of the pyramidal indentation
a	contact length of the pyramidal indentation
e	Engineering strain
f	Value of the objective function
F	Applied load in Vickers hardness test
k	Number of design variables
m	Friction factor
n	Strain hardening coefficient
P_a	Analysis penalty
P_k	Constraint penalty
w_1	Weighting factor of the constraint penalties
w_2	Weighting factor of the analysis penalty
a_1	Weighting factor of the material cost term of f
a_2	Weighting factor of the manufacturing cost term of f
a_3	Weighting factor of the shearing cost term of f
SF	Safety Factor
L0	Die Land
BT	Burr Thickness
H	Work piece height
L	Work Piece width
A1	Draft angle of the ribs
C1	Shearing force constant (0.85 for ductile materials)
C2	Shearing energy constant (0.5 for soft materials)
TS	Ultimate tensile strength.
f	Value of the objective function
P_a	Analysis error term
ε_o	Effective strain

ε_e	Representative strain
ε	True strain
σ_e	Representative stress
σ	True stress
η	Control term of the analysis penalty
σ_y	Yield Strength
σc	Cauchy stress matrix
$\dot{\varepsilon}$	Total elastic and plastic strain rate
α	Shearing angle

1. INTRODUCTION

There are mainly three aspects of the problem considered in this study, which are cold forging, optimization and concurrent engineering. In the last decades, cold forging has become one of the most widely used production methods due to its various advantages. Firstly, cold forming helps not only to produce parts of superior mechanical properties with better dimensional accuracy and surface finish, but also minimizes material waste compared to material removal processes. Moreover, forging to net or near net shape dimensions reduces the need for post processes, resulting in significant cost savings. On the other hand, because the tooling and equipment costs are relatively high, the process is feasible only if the part is to be produced in large numbers.[1]

Traditionally, manufacturing parameters are determined based on engineer's experience. In most cases, values for design parameters selected based on experience do not give satisfactory results. Thus, manufacturing parameters are modified according to outputs of a trial-error-correction phase. For manufacturing processes requiring high tooling costs, these trial and error efforts drastically decrease the efficiency of the product development process. The developments in the computer technology have changed this traditional approach. Numerical methods like FEM allows prediction of the effects of process parameters on the end product without actually producing it. This reduces trial and error efforts dramatically. On the other hand, FE analysis only provides outputs for a predetermined process; it cannot appraise these outputs and suggest a better process design. In most applications, the efficiency of the processing and the quality of the resulting product depend on various process and design parameters. Because FE analysis requires high computational costs, it is not feasible to determine the outputs for each set of values of these parameters using FE analysis. Thus a methodology is required to make viable decisions. Today, a variety of optimization techniques to be combined with FE analysis are available in the literature. In short, integration of optimization techniques with finite element analysis increases the effectiveness of the product

and process design. This integration allows reducing the design costs by shifting the burden from engineer to the computer. [2]

The forging process has a number of parameters that are under the control of the process designer, which can be used for process design optimization. By optimizing the controllable process parameters, one can improve the product quality, manufacturing efficiency or decrease costs significantly.

In order to identify the controllable process parameters, one needs to classify the process parameters systematically. A metal forging process is characterized by various process parameters that one may classify under two main divisions: mechanical process parameters and thermal process parameters. The mechanical process parameters are preform shape, die shape, die speed, die stroke, flow stress of the workpiece material. The thermal process parameters are initial temperature of the workpiece and dies, heat transfer coefficients including those at the die-workpiece interfaces, temperatures of the environment and cooling medium, thermal conductivity and heat capacity of the workpiece and die materials, lapse time between forming operations, thermal boundary conditions.[3]

According to the desired optimization aim, a suitable objective function is constructed. Choosing the objective and constraint functions and the optimization variables has paramount importance on the effectiveness and the reliability of the optimization. In the literature, different approaches were adopted in this respect.

Fourment and Chenot [4] used the total energy as a measure of the actual cost of the process in their metal forming optimization study. One of the advantages of choosing total energy as a criterion is that it is a rather smooth function of process design parameters, simplifying the optimization. In the same study, effective strain values were also used as a measure of the metallurgical quality of the forged part and these two indicators are combined in a single objective function.

Sonmez and Demir [5] used hardness distribution as a measure of part performance in use. The aim was to minimize the variation in hardness distribution in a backward extruded cup by optimizing die and preform shapes. Strain distribution was determined through a finite element analysis and an analytical relation between strain and hardness was used to determine the hardness distribution.

Ou *et al.* [6] used the disparity between the actual and desired forging shapes as a measure of quality for a forged product. In their study, forging errors due to die-elastic deformation, thermal distortion and press-elasticity were quantified in order to reveal distinctive dimensional and shape error patterns in a hot forging process for aerofoil sections. The FE results suggested that the inaccuracy in aerofoil thickness was mainly due to the die-elasticity and the aerofoil bow and twist errors, which depended on press deflections.

Gao *et al.* [7] considered the variance in grain size and the average value of grain size in the whole final product as a measure of microstructural quality and microstructural uniformity to formulate the objective function. Besides, two constraints were imposed on die underfill and excessive material waste. Two different types of design variables were considered in the study, including geometric parameters (initial shape of billet) and a process parameter (die velocity). By using a new approach based on sensitivity analysis for optimizing the microstructure development during the forging processes, the optimal initial shape of billet and the die velocity were obtained.

Very often, a part cannot be forged in a single operation; either the required forging force is too large, some forming defects may occur, or the microstructural properties of the final part are not satisfactory [8]. Then, at least two forging operations are often required in which several deformation paths may be considered. In the traditional approach, intermediate shapes are found through trial and error. Studies on process optimization of forging were usually devoted to preform optimization for different objectives like obtaining the exact shape by free forging [9]

In most of the classical optimization techniques, the gradients of objective functions are used to reach the solution; however, calculating the derivatives numerically poses difficulty. Besides, considering the difficult of modeling a manufacturing process by taking into account all factors and determining accurately the deformation and the changes in the temperature, the geometry, and material properties, and predicting the quality of the end product, it may not be possible to accurately determine the values of the objective and constraint functions. The error in the calculated derivatives will then be higher; in that case, the gradient methods may work. In order to overcome these difficulties, some methods were proposed. Kobayashi *et al.* [10,11] introduced the so-called 'backward tracing technique' and traced back the loading path in the actual forming process from a given final configuration. Another approach is to analytically compute the gradients of the objective function as adopted by Kusiak *et al.* [12,13] Because the perform shape optimization is not directly related to the context of this work, the detailed literature of the study is not presented thoroughly and just a glimpse of the idea is given to map the literature systematically.

As it is presented above, there are many examples of optimization of a specific phase like manufacturing or design phase. In this study, the concurrent approach is adopted in the optimization of product design and process design phases. In concurrent design, all steps of manufacturing are considered in the product design phase. This approach shortens the manufacturing cycle because all departmental needs are considered at the same time and there is no need for redesign at any stage of manufacture.

The long and costly lead times necessary in developing new forged products motivate the application of concurrent engineering principles and knowledge based computer software systems in forging [14]. In the traditional approach, because of the isolated product design and manufacturing phases, processing parameters that affect the manufacturing efficiency without affecting the performance of the product are not considered in the design phase even though values of these parameters are selected in the design phase. For example, it may be possible to manufacture a part in two stages, which can only be processed in three stages in its current design, by changing some of the preselected design parameters like fillet radii within the allowed range. In such a case, there are two options in the traditional approach. One option is

to modify the part design after becoming aware of the possibility that manufacturing cost can be decreased by changing the design; but this leads to a time cost and extra designing cost. The second option is to omit the redesigning option in order to keep the design cost minimum. This option has a kind of opportunity cost arising from accepting the already contributed extra manufacturing cost which may be eliminated by design modification.

There is only one study adopting a concurrent approach in forging process optimization. [14]; however it is rather a support software module development aimed at assisting manufacturing design decisions. This system combined theoretical and empirical knowledge about a variety of aspects of product design and manufacturing, and thus, it provided reasoning and decision-making capability for engineers in a way to decide parameters like material type, lubricant or machine type.

In the present study, the aim is to minimize specifically the overall cost of manufacturing by using some parameters of the product design, manufacturing, and post manufacturing design phases as optimization variables. The part to be optimized is an I-beam under centric load in a simply supported configuration. Nelder-Mead is chosen as the search algorithm and analysis is carried out using ANSYS Finite Element software.

2. PROBLEM STATEMENT

The aim of this study is to develop a concurrent design optimization methodology that can solve the combined optimization problem of product design and manufacturing phases. A cold forging process was chosen as the manufacturing process to be optimized.

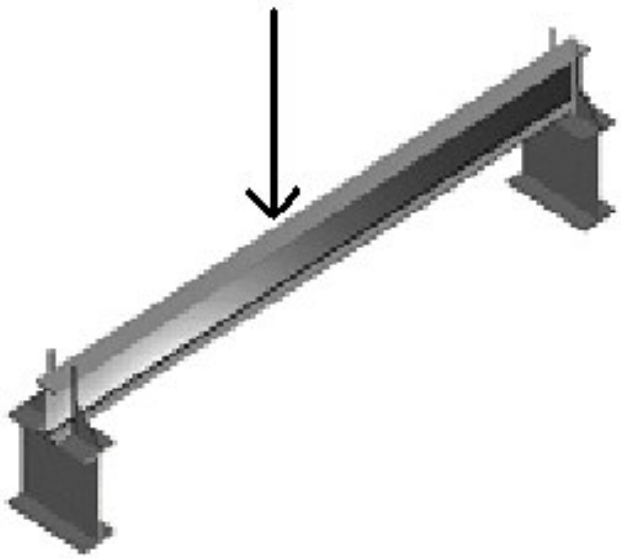

Figure 2.1. A schema of simply supported H-beam under a centric load.

The part to be optimized is a beam with an I-cross section that will be simply supported and subject to a centric loading as the worst loading condition during operation as shown in Figure 2.1. I-cross-sectioned beams are generally used in the industry for their good load carrying capacity under bending. For this reason, there have been many studies on choosing proper geometry, which may be useful to decide on the design parameters.

The manufacturing method of an I-cross section beam can be done either by forging or extrusion. The choice between extrusion and forging is made on the basis of manufacturing cost, mechanical properties desired and the length of the beam. The part in this study is

manufactured through forging followed by a shearing operation. As illustrated in Figure 2.2, the rectangular bar is firstly forged in to H-beam cross-section and this operation is followed by the shearing of the flashes.

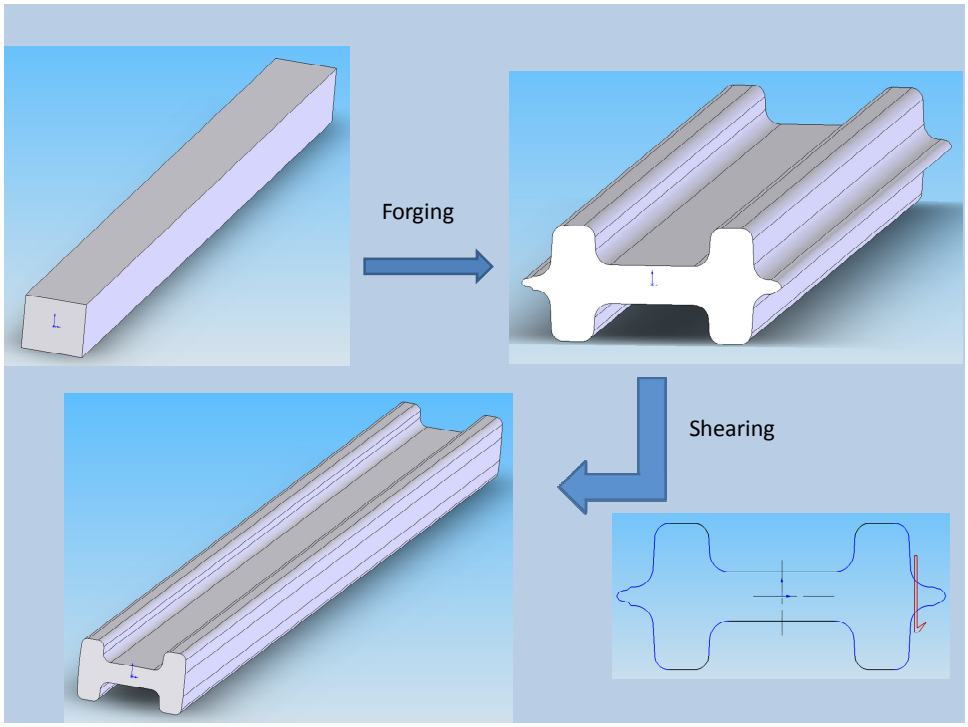

Fig 2.2 Manufacturing Phases of the H beam

.

Because I-beams are doubly symmetric, one of the representative quarters is used in the analysis as depicted in Figure 2.3. The main parameters focused in this study are radiuses R1 and R4, burr thickness BT and die land L1. Burr is the flash of the forged part to be cut off after forming. R1 and R4 are the radii of the fillets at the ribs of the I beam.

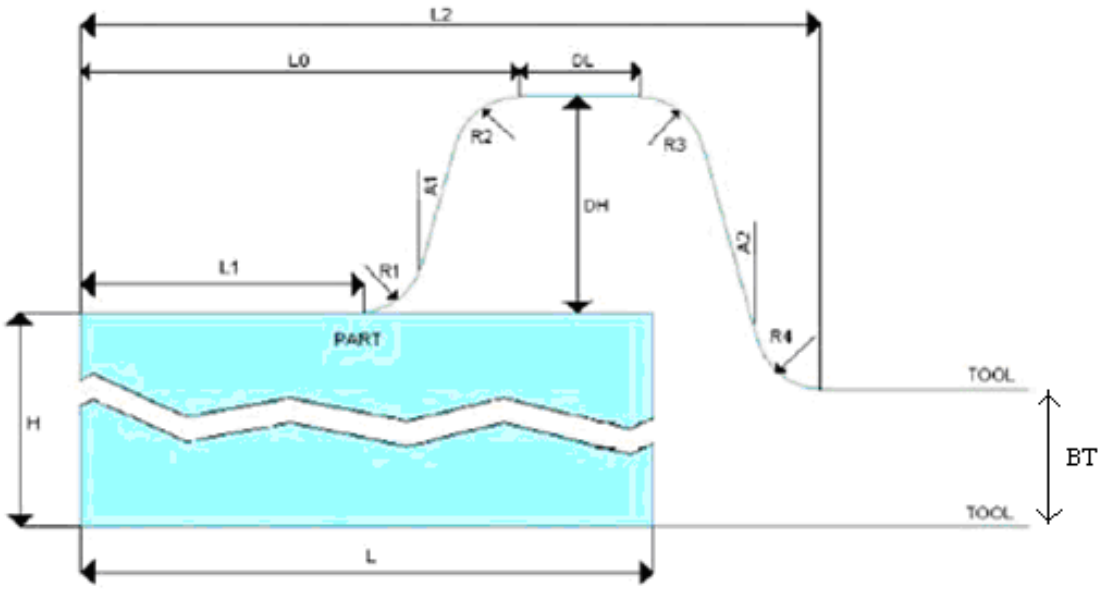

Figure 2.3. Design and manufacturing parameters of an H beam [15]

The objective of the optimization is to minimize the total cost depending on the chosen design variables with the condition that the part will not fail under the predefined working condition. Costs involving the design phase, manufacturing phase, and post-manufacturing phase are all considered. Accordingly, there are mainly three terms in the objective function:

- Part volume (for material cost)
- Total energy (for manufacturing cost)
- Shear energy of deburring (for post-manufacturing cost)

Effectiveness of the optimization process depends on the choice of the optimization parameters. In order to choose the most effective design parameters, a literature survey was performed. According to Khoury et al. [15], among the geometric parameters shown in Figure 2.2 burr thickness is the most effective one on the cost of forging energy. Besides, one should also consider its effect on the post manufacturing cost. By increasing the thickness of the burr, the mechanical energy required for forging decreases. On the other hand, a larger burr

thickness increases the energy needed for shearing. In this case a compromise should be made by choosing the suitable thickness that gives a lower value for the sum of the total strain energy and the cutting energy.

According to the study of Khoury et al. [15], after burr thickness, the second most effective parameters on the total strain energy are R4 and R1, which have about the same effect on strain energy. Considering the findings of the previous researchers, the parameters to be optimized were chosen as burr thickness-BT-, radiuses R1 and R4.

There is no effect of burr thickness on the strength of the part, thus on its failure during operation, because the burr will be cut in any way. Besides, the radiuses R1 and R4 have minor effect on the failure load because they have slight effect on the area moment of inertia of the cross section. Beside these variables, BT, R1 and R4, which do not affect the part performance, the die land L0, which affect the moment of inertia, thus the failure load, was chosen as optimization variable. R1 was taken to be equal to R4. Within the conditions stated above, there are three independent optimization variables in the problem considered in this study.

Structural optimization problems involve constraints on optimization variables in real life applications. For example, there may not be a feasible geometry corresponding to an arbitrary set of values for the optimization variables. Constraints define the feasible domains for variables. Selection of the constraint limits is usually based on the product requirements, the limitations on the manufacturing process or ergonomic considerations. If the feasible domain is arbitrarily restricted, better solutions may be missed or inapplicable solutions may be obtained. In this study, constraints are imposed on optimization variables based on the design or process requirements and possible instability sources in FE analysis. The constraints are listed in Table 2.1. The values and relations of the other geometric parameters are listed in Table 2.2:

Table 2.1. Constraint on the values (in mm) of the optimization variables.

$2 \leq$ RADIUSES 'R1=R4' ≤ 4
$1 \leq$ BURR THICKNESS 'BT' ≤ 8
$15 \leq$ DIE LAND 'LO' ≤ 19

Table 2.2. The values (in mm) and relations of geometric parameters.

DL=5
R2=R3=3
A1=A2=3
DH=10
H=16
L=18+(LO-18)/3

3. METHODOLOGY

The aim of this study is to develop a procedure to optimize the shape of an I-beam with a concurrent approach by considering design, manufacturing, and deburring phases to achieve minimum cost for the overall process. The cold forging process was analyzed through finite element modeling by using ANSYS package program and Nelder-Mead algorithm was used for optimization. Optimization variables are the die land, LO, rib radiuses R1 and R3, which are equal to each other, and burr thickness, BT, which are depicted in Figure 2.3. The I beam is formed by cold forging and the flash is sheared out as a post manufacturing operation.

3.1. Objective Function

An optimization procedure requires an objective function to be minimized which is expressed in terms of the optimization variables. In this thesis, the objective is to obtain the optimum geometric parameters for an I beam to minimize the total cost of the design, manufacturing and shearing phases.

There are mainly three parts to be calculated in the objective function of this study and one failure analysis.

$$f = \mathrm{MC} + \mathrm{FC} + \mathrm{SC} + \mathrm{P} \tag{3.1}$$

Where ‘MC’ is the material cost, ‘FC’ is the forging cost, ‘SC’ is the shearing cost and P is the penalty terms.

$$f = a_1.\mathrm{V} + a_2.\mathrm{FSE} + a_3\mathrm{SE} + \mathrm{P} \tag{3.2}$$

Where ‘V’ is the volume of the part, ‘FSE’ is the forging strain energy, ‘SE’ is the shearing energy and the a_i’s are the non dimensionalizing constants. The first term of the objective

function represents the material cost of the part. The second term represents the manufacturing cost of the part. The third term represents the post manufacturing cost of the part.

3.1.1. Material Cost Term

Material cost of a part is directly related to the part volume. By using this relation, part volume is used as a measure of material volume in the objective function. Because the third dimension remains constant during the processing, the material cost of the part is directly related to the cross sectional area. By considering the fact that volume does not change with the plastic deformation, the cross sectional area of the initial rectangular bar is simply used to estimate the material cost of the final product.

3.1.2. Manufacturing Cost Term

In this study, strain energy is used as a measure of the manufacturing cost of the part. In particular, forging strain energy is used as a term in objective function which is defined in Eq. 3.3.

$$FSE = \int_0^t \int_V (\sigma^c \dot{\varepsilon}\, dV)dt \tag{3.3}$$

where FSE is the forging strain energy, σ^c is the Cauchy stress matrix and $\dot{\varepsilon}$ is the total (elastic and plastic) strain rate. The expression in Equation 3.3 is not calculated analytically. The strain energy values are kept in the element tables of ANSYS and this value is used in the optimization. The ‘etable’ and ‘get’ commands are used in order to obtain the strain energy data.

3.1.3. Shearing Cost Term

Similar to the manufacturing cost term, shearing energy of the deburring process is used as a measure of the post manufacturing cost of the part. This term is calculated analytically by using the following formula: [16]

$$SE = C_2.C_1.(S_{ut}).h^2.\frac{h}{\tan\alpha} \tag{3.4}$$

where SE is the shearing energy, C_1 is a constant which is equal to 0.85 for ductile materials, C_2 is a constant which is equal to 0.5 for soft materials, h is the thickness to be sheared which is equal to BT in our case, α is the shearing angle which is chosen to be 6^o and S_{ut} is the tensile strength.

3.1.4. Weight Constants

The terms in the objective functions as presented above have different units. For this reason, they are not comparable. Because relative effect of individual terms may greatly affect the resulting design, using proper

Weighing constants for the terms in the objective function is important. The predefined common ground is chosen to be the cost ($) in our case. The objective function then becomes

$$f = a_1 \times V + a_2 \times \int_0^t \int_V (\sigma^c : \dot{\varepsilon}\, dV)dt + a_3 \times (TS).(BT)^3.\frac{C_2.C_1}{\tan\alpha} \tag{3.5}$$

where α_I are weighing constants. In order to decide on their values, a preliminary cost analysis was performed. It should be noted that the main scope of this study is to develop a concurrent optimization methodology not cost analysis, so the analysis done is just enough to

have some idea on the reasonable effects of the individual terms on the overall objective function.

There are mainly two units used in the objective function. The first term has the dimension of volume, the second and third terms have the dimension of energy. The conversion of volume to dollars can be expressed as

$$[\$] = Volume[cm^3] \times density[g/cm^3] \times unit\ price of\ the material[\$/g] \qquad (3.6)$$

The density of the material (ST37 Steel) is 7.85 g/cm^3 [17] and the unit price of the material is 650 dollars/ton [18]. According to the conversion above, the constant a_1 is calculated according to the Eq. 3.7 and used in objective function.

$$a_1 = density[g/cm^3] \times unit\ price of\ the material[\$/g] \qquad (3.7)$$

The other dimension to be converted to price is the energy. The local electricity price for industry is approximately 0.10 dollars/kWh. Assuming that electricity is converted to manufacturing energy with %50 percent efficiency, the cost of electricity spent during forging is calculated as

$$\begin{aligned} Electricity[\$] = Manufacturing\ energy[kWh] \times unit\ price \\ of\ electricity[\$/kWh] \times 0.50 \end{aligned} \qquad (3.8)$$

According to this conversion formula, the constants a_2, a_3 in Eq. 3.2 are calculated as

$$a_2 = a_3 = unit\ price of\ electricity[\$/kWh] \times 0.50 \qquad (3.9)$$

The costs that are independent of the design variables like labor, machinery costs are not included in the objective function.

3.1.5. Penalty Functions

During the optimization process, the value of the objective function is recalculated whenever the values of the optimization variables are changed by the search algorithm. For this purpose, non-linear FE analyses involving large deformation are performed in every step of iteration.

One of the problems that may occur is the failure of analysis and to be stuck at a fake minimum point. The search algorithm may generate a set of variables such that for some reason FE analysis fails, e.g. the geometry may not be constructed due to a negative value for radius of curvature. In that case, the value of the second term of the objective function, which is calculated by ANSYS, will be zero. Consequently, the algorithm obtains zero manufacturing energy and it sticks into this fake minimum point. In order to prevent this, an analysis error term, P_a, is defined. This error term should have a large value compared to other terms in the objective function so that it prevents converging into a fake minimum point. The analysis error term P_a becomes active, if FE analysis fails. P_a is used with a control coefficient η. In such a case, η is equal to 1.0 and the third term becomes nonzero. Otherwise, η is equal to zero.

Another problem that may occur during optimization is the case that the algorithm assigns a value to a design variable that violates the constraint conditions, which does not necessarily end up with analysis failure.

Suppose that for the selected optimization variable, x, there exist a lower and an upper bound denoted by x_l and x_u respectively. The inequality constraint is expressed as

$$x_l < x < x_u \tag{3.10}$$

This relation requires that two penalty functions be defined. For the lower bound, the penalty function is defined as

$$P_k = \left\langle \frac{-x + x_l}{x_l} \right\rangle \tag{3.11}$$

and the penalty function for the upper bound as

$$P_{k+1} = \left\langle \frac{x - x_u}{x_u} \right\rangle \tag{3.12}$$

Because the type of the penalty functions is external, they become active if their related constraint is violated. Otherwise, they are equal to zero. This activity is controlled by the operator "< >". If the value of the term inside this operator is positive, it yields the same value, otherwise it yields zero. Note that all of the penalty functions are defined in a manner such that they become less than zero if their related variable takes a value within its feasible range. [19]

In this study, there are three optimization parameters, on which both upper and lower limits are imposed. Besides, In addition to the objective function terms, one more expression is calculated in order to check the failure case of the part within the working conditions. The maximum Stress occurred through the part is found by using the pure bending formulation of a centric loaded a simply supported beam [20]. This stress value is then compared with the yield stress of the material by taking the safety factor into account and if the failure condition is satisfied, penalty term in the objective function is activated. Consequently, 7 penalty functions are used in this study.

The final form of the objective function can then be given as

$$f(R1, R3, BT, L0) = a_1 \times Volume + a_2 \times \int_0^t \int_V (\sigma^c : \dot{\varepsilon}\, dV)dt + a_3 \times (S_{ut}).(BT)^3.(4.0476) + w\sum_{k=1}^{7} P_k + \eta P_a \quad (3.13)$$

The objective function in this form includes terms related to the efficiency of the manufacturing as well as to the effectiveness of the design. The seventh penalty function ensures that the part will not fail when it is put into use. Through the use of the first and the second terms, the manufacturing cost is minimized. Consequently, the objective function reflects the concurrent design aspect.

3.1.6. Yield Strength Calculation after Cold Work

The yield strength, σ_y, of the undeformed material used in the forging, St37 Steel, is 250 MPa. [17] Using this value as the yield strength in the failure criterion for the working condition is not realistic because there is a prior work hardening on the material through the forging process. The procedure to estimate the new yielding stress is as follows

- The locations where failure is expected to occur are determined.
- The true stresses at these locations are obtained from the ANSYS results
- The true stress is converted to engineering stress.

The locations where failure is expected for our part is the top line of the I beam, which is denoted by a red line in Figure 3.1. This is because the maximum stress, Mc/I, occurs in this region..

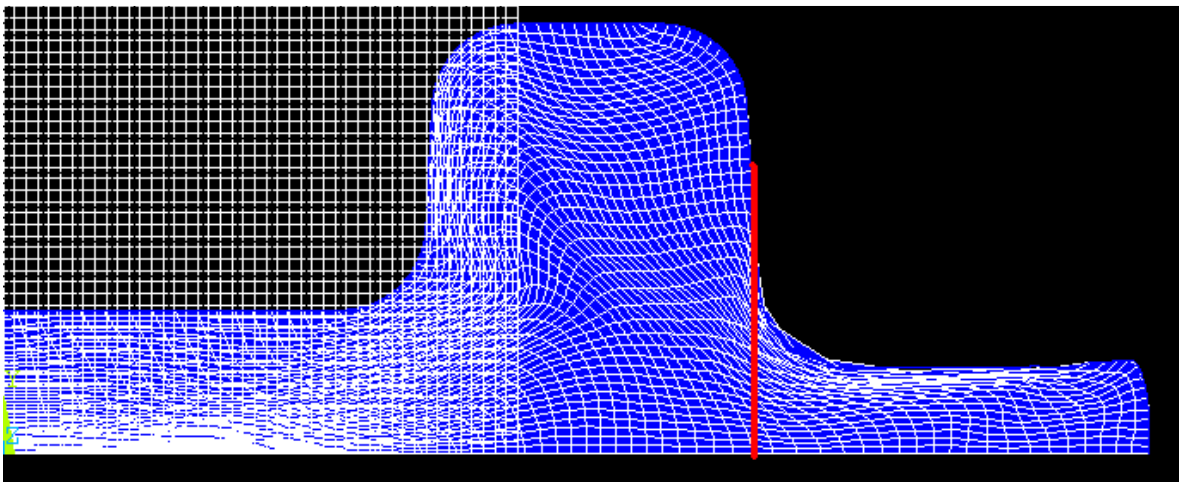

Figure 3.1. Possible failure line for the I beam

After the manufacturing process is simulated through ANSYS, the equivalent stresses along this line is obtained as shown in Figure 3.2. Based on the date, an average value of 520 MPa is chosen to be the reference true yield strength for the work hardened material.

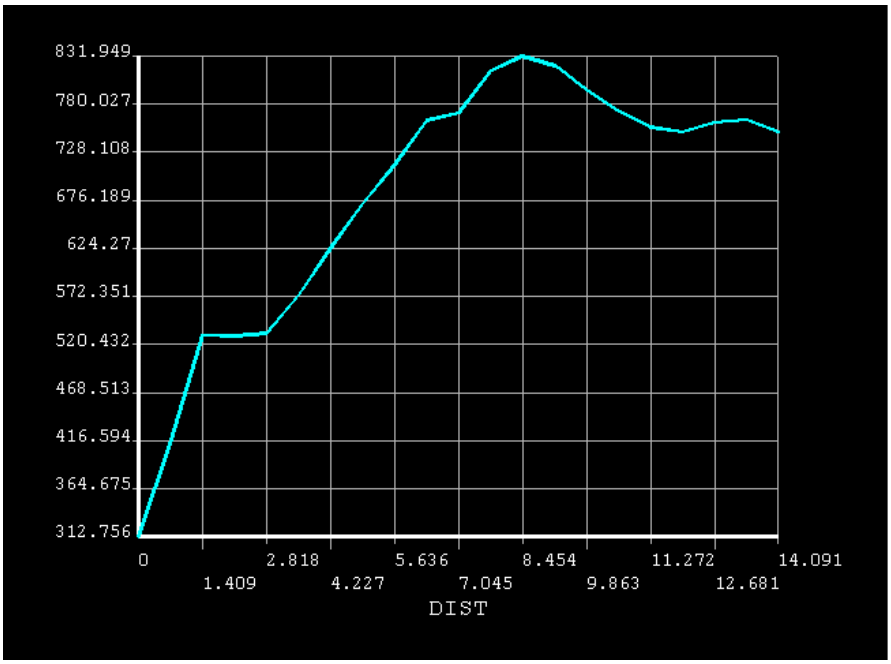

Figure 3.2 Post manufacturing stresses on I beam head line

The conversion between true stress and engineering stress is done by using the following equation:

$$\sigma_E = \frac{\sigma_T}{e^{\varepsilon_T}} \tag{3.14}$$

where σ_T is the true stress, ε_T is the true strain, σ_E is the engineering stress. The true strain is obtained from the MISO flow curve of St37 shown in Fig. 3.10. The true strain corresponding to 520 MPa true stress is 0.1. According to the equation above, by using the true stress-strain value, engineering stress is found to be 470 MPa.

3.1.7. Structural Analysis

According to the concurrent engineering design approach, the mechanical design phase for working conditions is coupled with the manufacturing design phase. Accordingly, the engineering analysis of the part to be designed according to the working conditions is carried out and cost of the design is incorporated into the objective function.

The contribution of this aspect of the problem to the objective function is in the form of a penalty function. The expression added to the objective function is calculated in a way that if the part to be designed with the given parameters fails under the working conditions, a penalty value is added to the objective function in a way that this configuration of the part is to be regarded as unfavorable by the optimization algorithm.

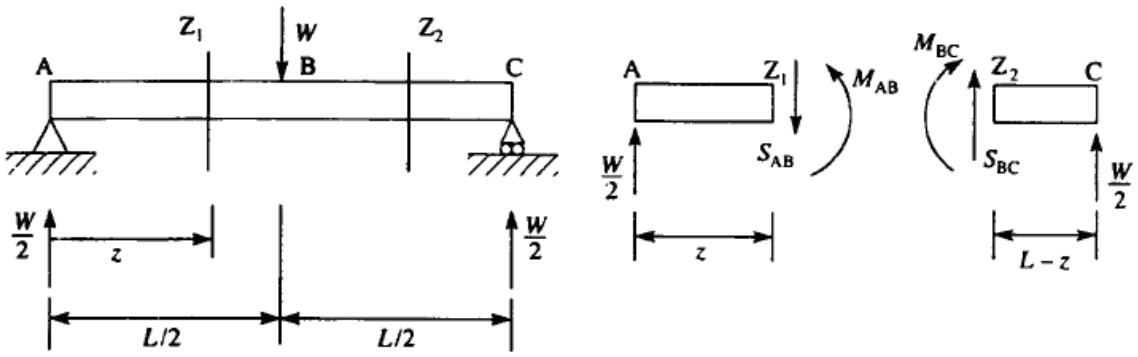

Figure 3.3. Loading condition and section forces.[20]

In order to calculate the maximum stress in the simply supported beam, a moment analysis is done. The simplified diagram and the sign conventions used in the calculations are shown in Figure 3.3.

According to the force equilibrium in the vertical direction and moment equilibrium, the maximum bending moment is found at z=$\frac{L}{2}$ as

$$M_{\max} = \frac{WL}{4} \tag{3.15}$$

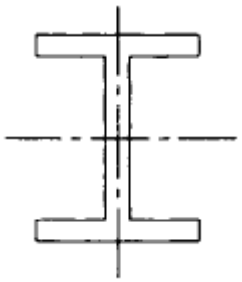

Figure 3.4. Double Symmetric I-beam cross section.[20]

The I beam considered in our problem has a double symmetrical cross-section as seen in Figure 3.4. The material is assumed to be linearly elastic and homogeneous. Bernoulli-Euler

beam theory is supposed to be valid for stress calculations considering that the length of the beam is large in comparison to cross-sectional dimensions. .

The normal stress developed in the beam due to bending can be stated as

$$\sigma_z = \frac{My}{I_x} \tag{3.16}$$

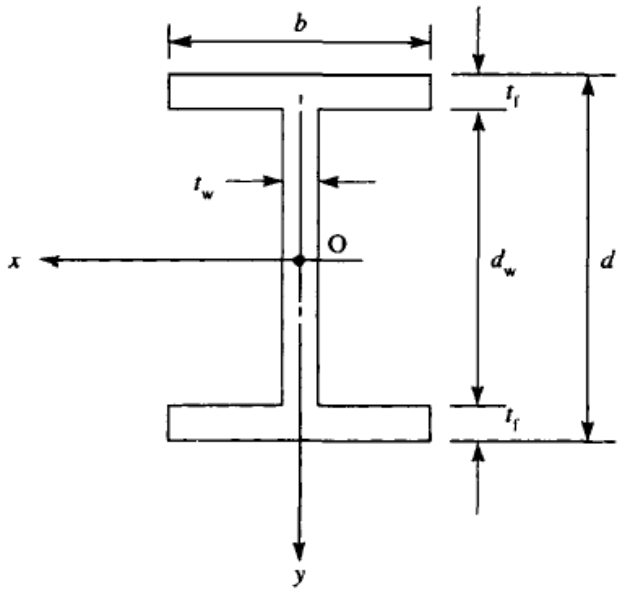

Figure 3.5. I beam parameters[20]

The area moment of inertia of an I-beam with the cross-sectional dimensions shown in Figure 3.3 is given as [20]

$$I_x = \frac{bd^3}{12} - \frac{(b-t_w)d_w^{\,3}}{12} \tag{3.17}$$

It should be noted that the I-beam used in our analysis is not exactly the same as the one shown in the Figure 3.3. The I beam studied have curved surfaces at the rib corners and

web intersections with the given radii, which are denoted as R1, R2, R3, R4 in the problem description and depicted in Figure 2.2. Besides, there is a slight draft angle, A1 or A2, on the ribs for the sake of manufacturability, which was taken as 3°, and it is assumed to have negligible effect on the stress.

After the expressions for M and I_x are plugged in Eq. 3.14., the maximum stress for y = d/2 turns out to be

$$\sigma_{\max} = \frac{\frac{WL}{4}.y}{\frac{bd^3}{12} - \frac{(b-t_w)d_w^{\,3}}{12}} \tag{3.18}$$

When the parameter values are substituted into Eq. 3.18, the maximum stress is expressed in terms of L0 as

$$\sigma_{\max} = \frac{\frac{22000.500}{4}.(L0+8)}{\frac{30.(2L0+16)^3}{12} - \frac{(30-10)(2L0-6)^3}{12}} \tag{3.19}$$

If the unit of L0 is taken to be mm

$$\sigma_{\max} = \frac{3300000(L0+8)}{3.(2L0+16)^3 - 2.(2L0-6)^3} \ [MPa] \tag{3.20}$$

The critical point is under the uniaxial stress in the z direction. For this reason, the empirical failure criterion for yielding under the uniaxial load is used.

$$\sigma_{\max} \geq \frac{\sigma_y}{SF} \tag{3.21}$$

Assuming that the working conditions of the part do not involve high uncertainties, the safety factor, SF, is chosen to be 2.0. When all these values are substituted, the failure criterion becomes

$$14042 \geq \frac{3.(2L0+16)^3 - 2.(2L0-6)^3}{(L0+8)} \tag{3.22}$$

If this criterion is met, the penalty function is activated and a penalty value is added to the objective function. The penalty value chosen for a failure case is 50. When this value is compared with the typical values of the objective function during optimization, which is in the range of 3-4, it is obvious that the penalty added is large enough to avoid from failure cases.

3.2. Optimization Procedure

Definition of an optimization problem requires

- Determination of the objective function to be minimized
- Selection of design variables affecting the value of the objective function and the penalty functions.
- Setting the constraints
- Defining penalty function, weighting constants
- Selection of the search algorithm.

In this study, Nelder-Mead algorithm was selected as search algorithm because it is a robust zero order search algorithm not requiring numerical derivatives of the objective function. The finite element model and the optimization algorithm are integrated by using a built-in ANSYS code. This program carries out FE analyses, writes the results into output files, and also evaluates the results to modify the optimization variables according to the decision criteria of the Nelder-Mead algorithm.

Figure 3.6 shows the flow chart of the methodology followed in this study. The details of the finite element analysis and the optimization procedure are explained in the related sections.

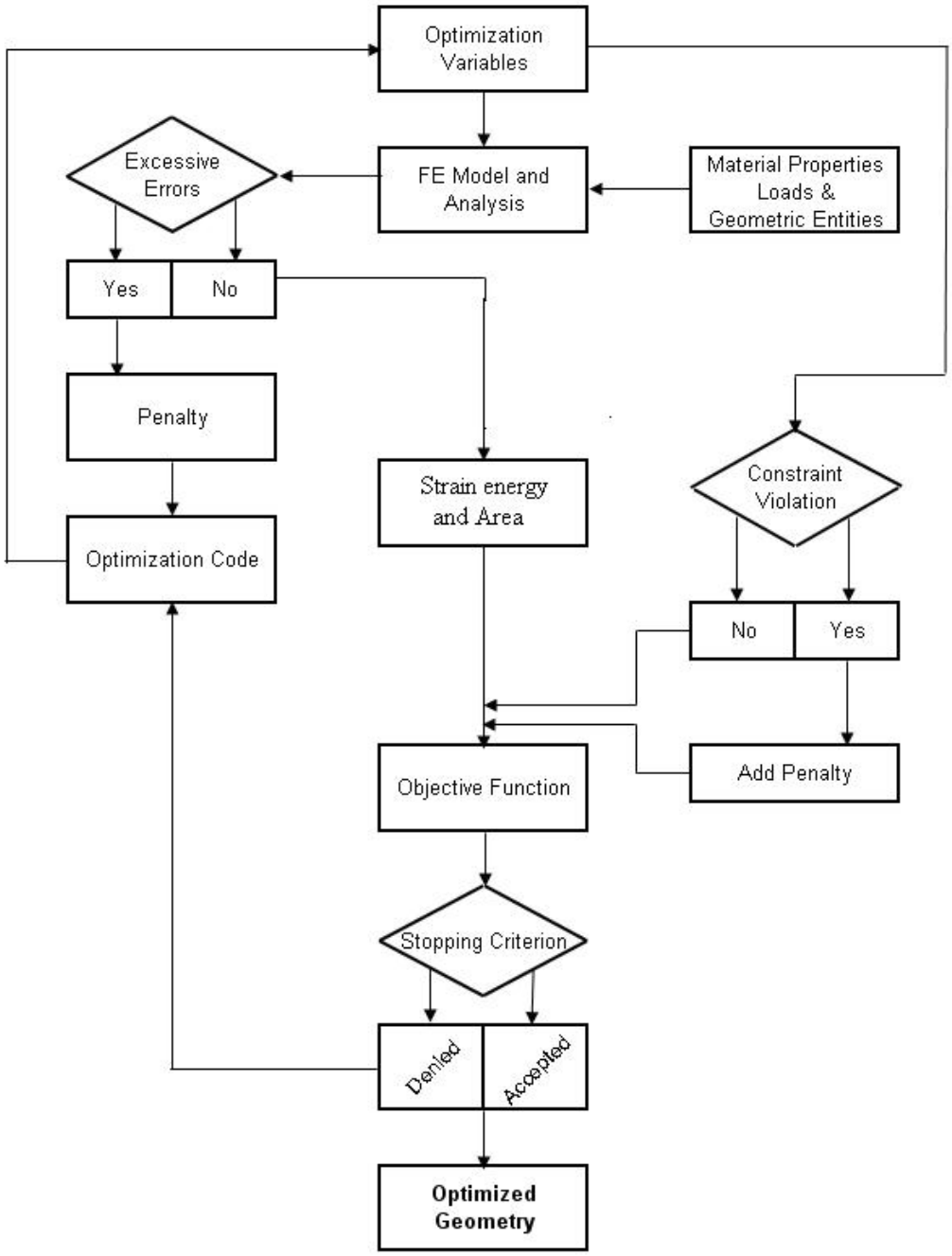

Figure 3.6. The flow chart of the optimization process

Initially, the optimization code selects random values for the optimization variables within the feasible domain and creates an initial geometry accordingly. Then, the predefined loads and boundary conditions are applied on the finite element model and a finite element analysis is conducted using the chosen material properties to obtain the total strain energy and part area. By using the data obtained from the finite element analysis, the objective function terms are calculated. These values are multiplied by the weight constants which make these terms non-dimensional and comparable in magnitude. The details of the calculation method for the objective function terms and the weight constants are given in the following sections.

As mentioned before, the objective function is defined as the sum of a number of terms multiplied by their weight constants. Because, there are constraints on the optimization variables, this is a constrained optimization problem. In cases of constraint violations, a penalty is calculated and added to the value of the objective function. In this way, the problem is transformed to an unconstrained optimization problem.

Another penalty case is activated if the given configuration of the part fails under the working conditions. The maximum equivalent stress calculated based on the operating conditions is used to decide on whether failure will occur or not according to the failure criterion.

Penalties are activated under three conditions:

- If an optimization variable takes a value outside its feasible range
- If the given configuration fails under the working conditions defined in the problem
- If the FE analysis fails.

Further details of the penalty method are given in the following sections. Because the Nelder-Mead Algorithm requires k+1 configurations, k being the number of design variables, this procedure is repeated for four randomly created initial configurations. Having completed four FE analyses and obtained objective function values, the program compares these values according to the decision criteria of the Nelder-Mead Algorithm. This comparison leads to

calculation of new values for the optimization variables and creation of a new geometry to be analyzed. In the Appendix B, the Nelder-Mead algorithm is explained in detail. This procedure is repeated until the stopping criterion is satisfied, which requires the difference between the objective function values of the best and worst configurations to be small. [19]

3.3. Finite Element Modeling

Figure 3.7 shows a geometric representation of the die profile and workpiece in ANSYS. Owing to the doubly symmetric cross-section, a two dimensional model under plane strain conditions is used instead of creating a 3D model in order to reduce the computational effort.

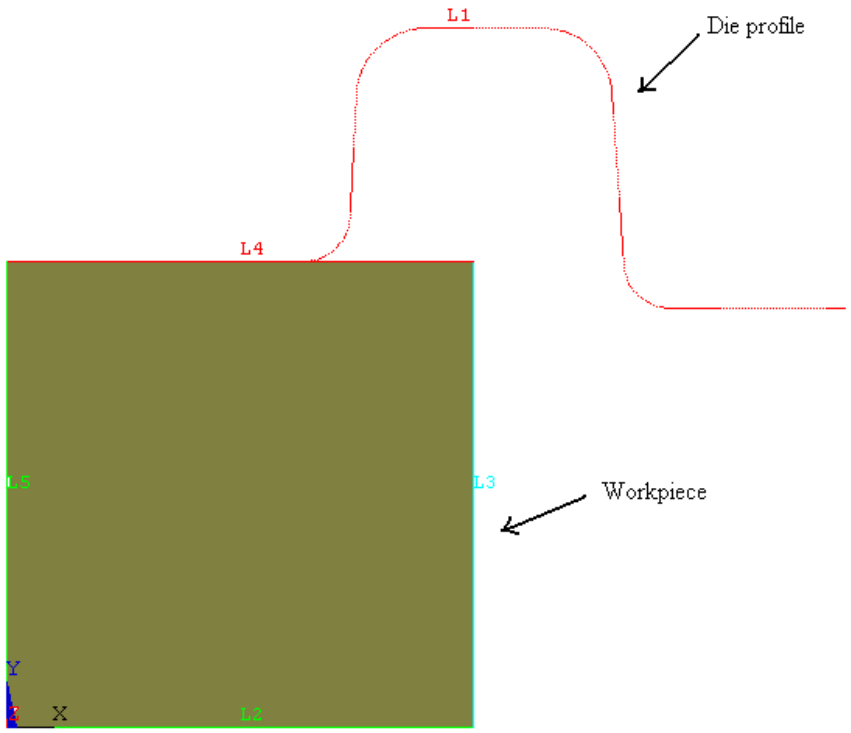

Figure 3.7. Workpiece and die profile lines in ANSYS.

During the optimization, the FE model is created using batch files and a fully parametric geometry design is done for simple integration with the optimization code. In this way, the FE

analysis is carried out and current optimization values are selected according to the search algorithm in each iteration through a single program without user intervention.

3.3.1 Meshing and Elements

Selection of an appropriate element type in the analysis is essential for obtaining reliable results. Selected element should satisfy a set of requirements: Firstly, the element should be suitable for 2D modeling of the structure. Secondly, the element should have large deflection, large strain capabilities because of high deformation behavior of the workpiece. Lastly, a high order element is more suitable for highly nonlinear deformation process like cold forging. By considering all these requirements, the element type selected in this study is Plane183 (Figure 3.6), which is a high order, 8 node 2D rectangular element.

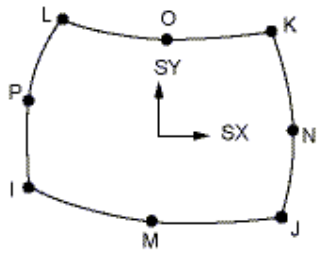

Figure 3.8 PLANE183 with its 8 nodes [22]

3.3.2 Contact Elements

Assuming that the die and the punch do not undergo plastic deformation and their elastic deformations have a negligible effect on the deformation of the workpiece, their surfaces were defined as nondeformable by using rigid lines surrounding their representative areas, and thus they were not meshed. Only the workpiece was meshed and a meshed contact is defined between the rigid punch and workpiece. Consequently, the number of mesh elements to be evaluated during the analysis is reduced, and the required solution time is decreased.

The contact type used in this study is rigid-to-flexible and surface-to-surface contact.

The dies and punch are defined as rigid target bodies whereas the workpiece is a deformable contact body. In order to establish contact pairs between the punch and the workpiece, the boundary lines of the bodies are meshed.

Under the conditions defined above, CONTA172 was selected for deformable lines, and TARGE169 was selected for non-deformable lines in the analysis. The final shape of the meshed workpiece, contact pairs and the boundaries are depicted in Figure 3.9. The major contact is between line L1 and L4 (Fig. 3.9) which is defined as a rigid to deformable contact.

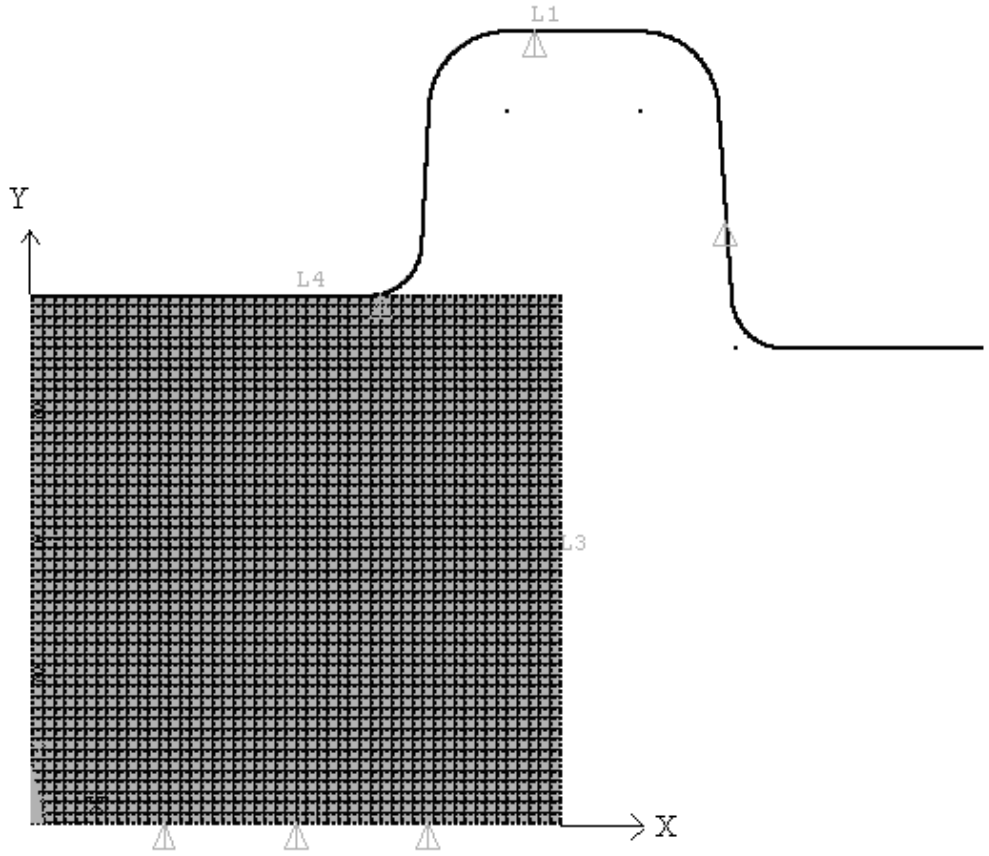

Figure 3.9. The FE model with its mesh, contact pairs and boundary conditions

3.3.3 Boundary Conditions

Regarding the boundary conditions, there are only displacement boundary conditions applied on lines and nodes. Symmetry boundary conditions are defined on lines L2 and L5. The punch line is restrained from moving along the *x*-axis and rotation. They are only allowed to move through the prescribed vertical displacement which is 15mm in –Y direction.

3.3.4 Friction Coefficient

In the literature, one of the proposed methods to determine the friction coefficient for die-workpiece interface was to conduct ring compression tests. Gouveia et al. [23] conducted FE simulations of forward extrusion process. They used Coulomb friction model with a constant friction coefficient of 0.18, which was obtained by ring upsetting experiments. Experimental measurements were not in agreement with the finite element analysis in this work. The disagreement was explained by differences in the deformation behavior of the material in upsetting and extrusion and the pressure differences, and they also stated that applying a lower friction coefficient would give theoretical results closer to that of experiments.

Hur et al. [24] simulated backward extrusion process. The friction coefficient *m* was assumed to be constant and equal to 0.1. Petruska and Janicek [25] studied strain inhomogeneity through hardness measurements on cold formed products. The type of the forming process they considered was forward extrusion. They simulated friction by Coulomb's model, and the friction coefficient was equal to 0.15. Roy et al. [26] simulated extrusion process of automotive outer race preforms. They applied a constant friction coefficient of 0.1 in their FE model.

In this study, Coulomb's model was assumed to correctly reflect the friction at the die-workpiece interface as in the previous studies. However, there is no clear agreement on the value of the friction coefficient *m*. In practice, friction coefficient may depend on the type of the materials in contact, but it may also vary due to varying lubrication and surface conditions

even if the same types of die and workpiece materials are used. In this study, the friction constant was assumed to be 0.15, which was within the range of values adopted in the previous studies. [19]

3.3.5 Material Model

Among the several alternatives to model the material properties in ANSYS, the selected material model is multi-linear isotropic hardening (MISO) model. MISO is a rate independent model suitable for large strain applications.

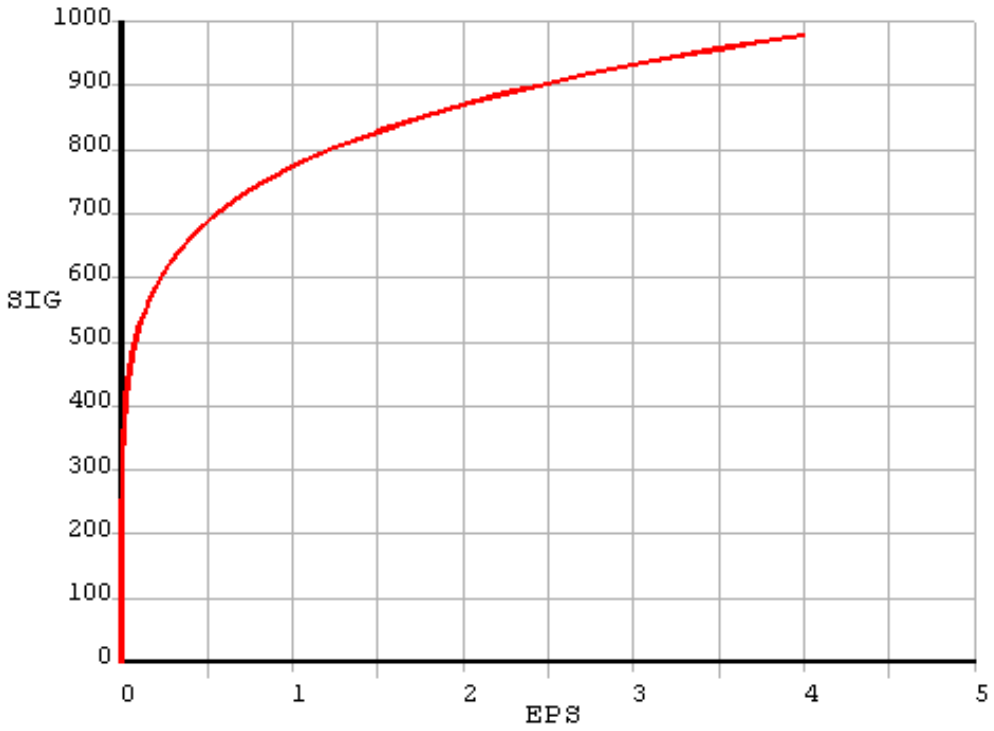

Figure 3.10. MISO flow curve of St37 generated in ANSYS.

In MISO, the stress-strain curve is described by a set of linear sub-elements, instead of a power equation. To define the strain-stress curve to be used in the nonlinear analysis, datum points from the stress-strain curve are required. The more points are entered, the better the non-linear behavior is approached. The MISO flow curve of ST37 created by ANSYS using

the given points is shown in Figure 3.10. This curve is defined by 38 datum points from the materials flow curve. These points are given in Appendix A.

3.3.6 Convergence Analysis

In finite element analysis, having some numerical results from the program does not necessarily mean that the results are reliable. Because accuracy of the solution depends on some settings like element size or number of substeps, a refinement of these settings should be done to find the effective and feasible choices for these settings.

Although the program itself guides the user by some warning messages like excessive deformation, one may not solely rely on these messages. One of the ways of choosing appropriate settings is to carry out a convergence analysis. In convergence analysis, user chooses a reference result parameter to see the dependence of that parameter to the settings of the program coded. When the dependence converges to an acceptable value, the settings used are regarded as appropriate.

In this study, maximum von Mises stress and maximum von Mises strains were chosen to be the control result parameters. Firstly, a suitable number of substeps is sought. Starting from 750, different substep numbers are tried using different element sizes ranging from 0.3 to 1. Up to the substep number of 2000, program gave some excessive deformation warnings especially in the small element size runs. Thus, the substep number is set to be 2000.

Secondly, to find the optimum value of element size, runs are given for element sizes 1, 0.7, 0.6, 0.5, 0.4, 0.3. Table 3.1 shows the results of the runs for these element sizes and the corresponding % percentage differences.

Table 3.1. Maximum von Misses stresses and maximum von Misses strains corresponding to different element sizes

Element Size	Max Von Misses Stress	% Difference	Max Von Misses Total Strain	% Difference
0.3	878.326000	0.007743	2.113000	0.047348
0.4	878.258000	0.028360	2.112000	0.142248
0.5	878.009000	0.024493	2.109000	0.142450
0.6	877.794000	0.053344	2.106000	0.333492
0.7	877.326000	0.163833	2.099000	0.962001
1	875.891000		2.079000	

The results are also demonstrated in Fig. 3.11 and Fig. 3.12, which show the relation between element size and maximum von Misses stress and maximum von Misses strain. As it can be seen from the figures, the element size of 0.4, for which the values are settling, seems to be an acceptable value for element size for both of the control result parameters chosen.

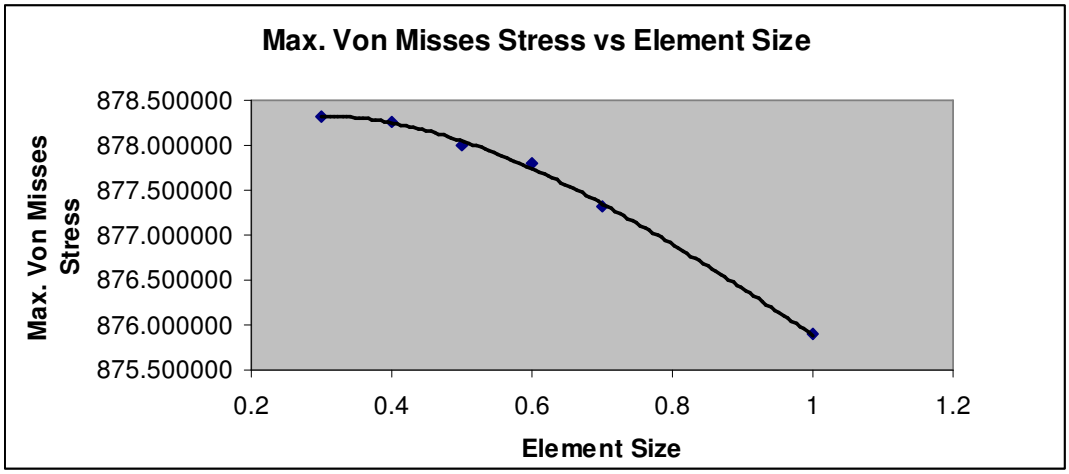

Figure 3.11. Maximum von Misses stress vs. element size graph.

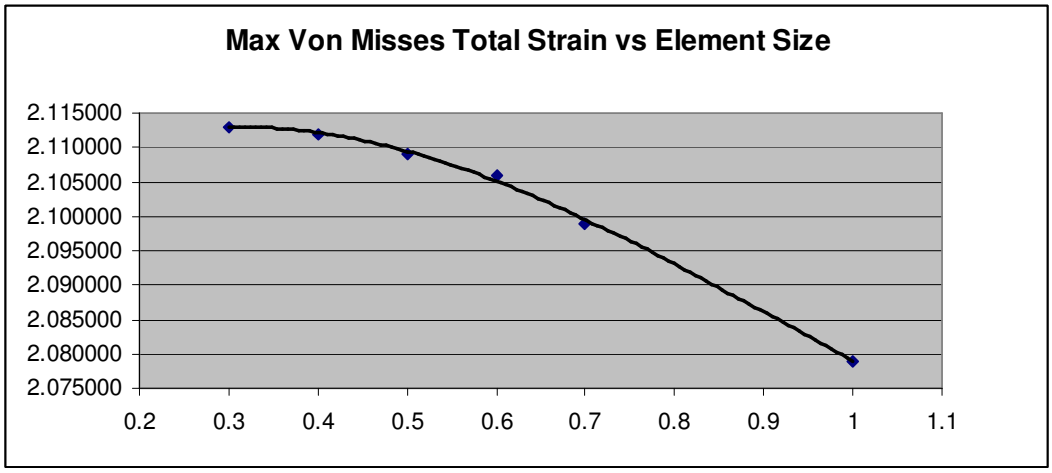

Figure 3.12. Maximum von Misses strain vs. element size graph.

A sample analysis is done using the settings found suitable after the convergence analysis. Some representative stages of the analysis are depicted in Figures ….

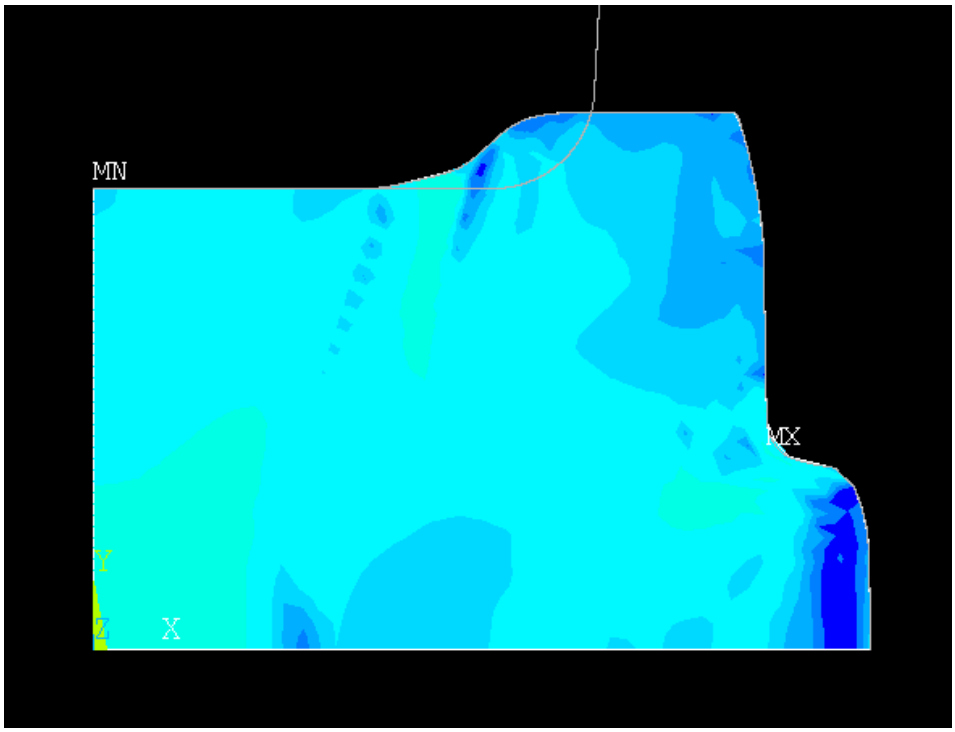

Figure 3.13. Depiction of a middle stage from the analysis.

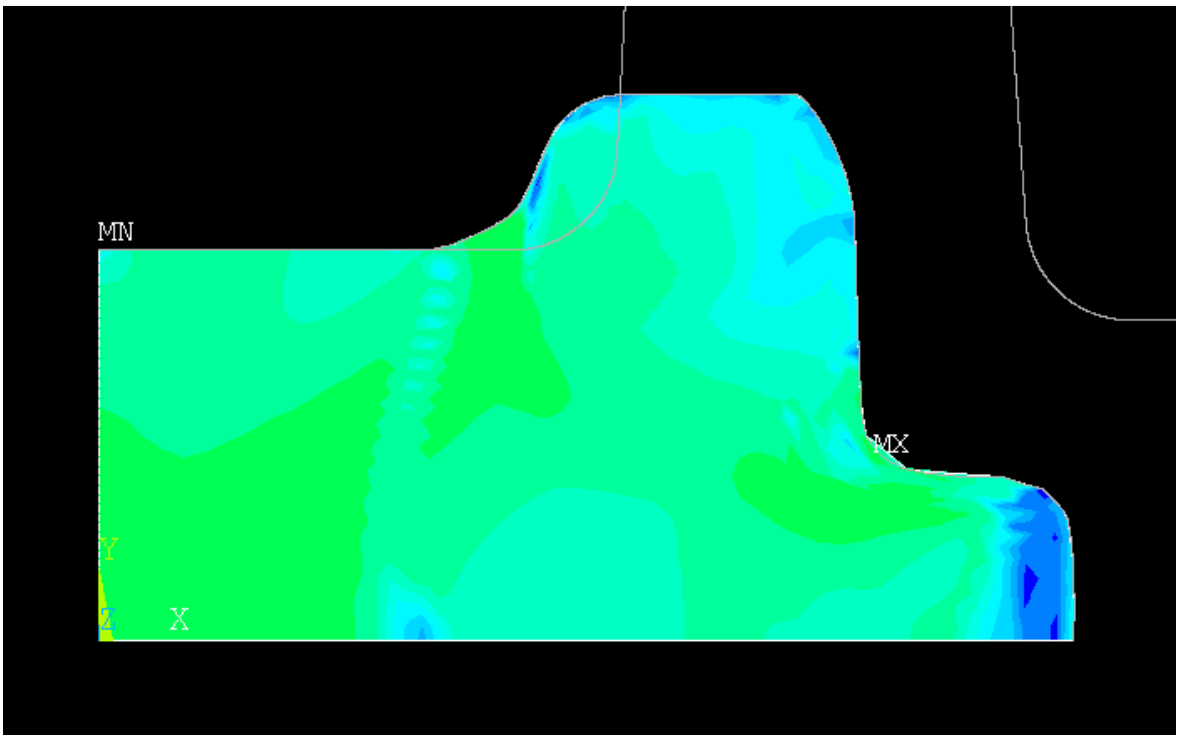

Figure 3.14. Depiction of a middle stage from the analysis.

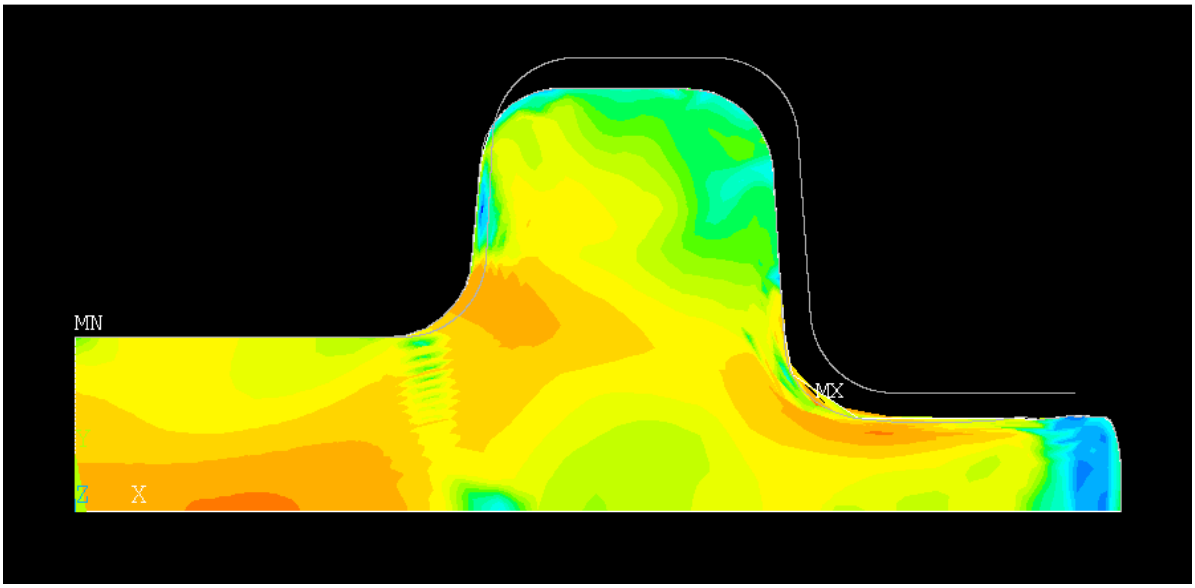

Figure 3.15. Depiction of a middle stage from the analysis

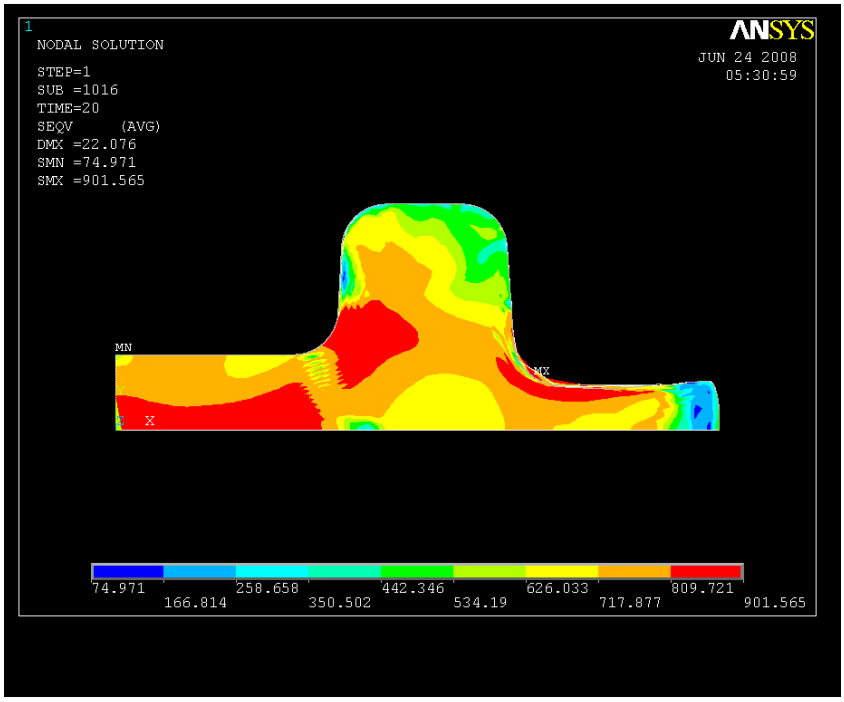

Figure 3.16. The final shape and the equivalent stress distribution.

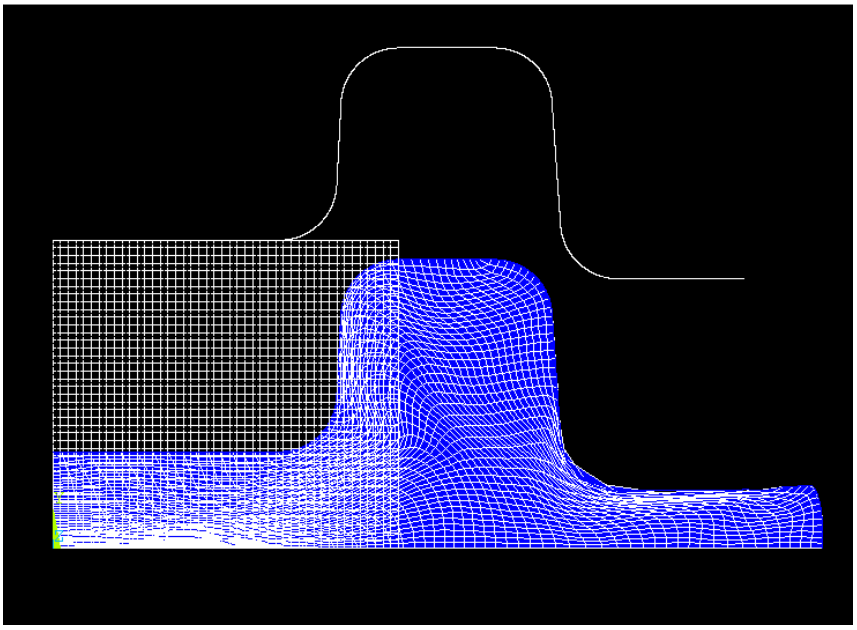

Figure 3.17. The meshed view of the deformed and undeformed shape of the part

4. RESULTS AND DISCUSSIONS

There are mainly four phases in this study regarding optimization. Firstly, the optimization is done for two variables; either with R1-R3 and the burr thickness-BT or die land L0 and burr thickness-BT without using the working condition failure criterion. Secondly, the die land is added as an optimization parameter and another set of runs are done. Finally, the working condition failure criterion is added to the three variable optimization and final results are obtained.

Dividing the work into phases is advantageous in two ways. It helps to proceed in the research in a more conscious manner by being able to diagnose problems in a better way. Besides, it gives more perspectives to draw conclusions about the effects of the lately added conditions by comparing different cases.

Because a number of local optimum points may exist, the optimization runs were repeated at least two times, starting from different initial values of optimization variables.

Two different cases are compared in the two variable optimization case. Firstly, optimization is done for the two variables; die land L0 and burr thickness-BT without using the working condition failure criterion. The lower and upper limits defined for L0 is 15 and 19 respectively. Similarly, the lower and upper limits defined BT is 1 and 8 respectively. The resulting optimal values of the variables are presented in Table 4.1.

Table 4.1. Results of die land, L0, and burr thickness, BT, optimization.

	Burr Thickness BT	Die Land L0	Objective Function Value *f*
1st Set	4.284	16.281	1.330
	6.549	17.329	1.536
	5.866	15.280	1.404
Last Set	1.254	15.097	1.239
	2.107	15.410	1.243
	1.645	15.528	1.242

In Table 4.1, the data sets between the first and the last set are not included for space considerations. As it can be seen from the table, the objective function values, which represent the overall cost of the processes, decrease through the iterations and end up with the minimum value of 1.242.

The second optimization was performed using the radius R1 and burr thickness, BT, as optimization variables without working condition failure criterion. The range of permissible values for R1 is from 1 to 5 and for BT is from 1 to 8. The resulting optimal values of the variables are presented in Table 4.2.

Table 4.2. Results of radius R1 and burr thickness, BT, optimization.

	Radius R1=R3	Burr Thickness BT	Objective Function Value *f*
Last Set	1.030	4.107	1.319
	1.581	4.165	1.322
	1.528	3.715	1.317

As it can be seen from the objective function values of the two cases, the effect of L0 on the overall cost is larger than the effect of radiuses R1 and R3. Using L0 as a control parameter with burr thickness is approximately 6% more effective on the overall cost.

Then optimization was performed using three variables without introducing the working condition failure criterion. The range of permissible values for R1 is from 2 to 4, for BT is from 1 to 8 and for the die land is from 15 to 19. The results of this optimization are given in Table 4.3.

Table 4.3. Results of the optimization with the variables die land, L0, radius R1 and burr thickness, BT.

	Burr Thickness BT	Radius R1=R3	Die Land L0	Objective Function Value *f*
Last Set	2.134	3.811	16.082	1.286
	2.577	3.627	16.495	1.288
	1.462	3.922	16.334	1.272
	1.123	3.808	17.022	1.290

The first conclusion drawn from this optimization by comparing the results on Table 4.3 to the previous two parameter cases is that the major variable that is dominant on the cost is the die land and it is tending to have smaller values at the optimal case. This is something more obvious when the nature of the objective function is further considered.

The objective function consists of three main terms which are material cost term, manufacturing cost term and the shearing cost term. In order to understand the effects of these terms on the overall cost, a sample analysis is carried out for one iteration and presented in Table 4.4.

Table 4.4. Effects of three cost parameters on the overall process cost

	Material cost term	Manufacturing cost term	Shearing cost term
Direct contribution to objective function value	1,18	0,0772	0,181
Percentage contribution to objective function value	81,84	5,35	12,55

The major result that can be drawn from Table 4.4 is that the major effect on the overall cost of the process is the effect of the material cost. It should be also noted that the non-recurring costs like machinery cost or manufacturing plant rental is not added to the manufacturing cost. In order to make an absolute conclusion about this issue, one should also take them into consideration because these additional cost terms are only effective on manufacturing and shearing costs which will not change our optimization results but may change the percentage distribution.

The die-land has dominant effect on material cost term and slight effect on the manufacturing term. Burr thickness has effects on manufacturing term and the shearing term. Radius has slight effect on material cost term and manufacturing term. As the major effective parameter on the most effective term, die land has a significant effect on the overall cost.

The last phase of the optimization is to take into account the working condition failure criterion in the objective as a penalty term or as a new constraint. The results of this condition are presented in Table 4.5.

Table 4.5. Results of the optimization with the variables die land, L0, radius R1 and burr thickness, BT, including part failure criterion.

Burr Thickness BT	Radius R1=R3	Die Land L0	Objective Function Value *f*
1.140	3.910	18.820	1.343
2.346	3.517	18.379	1.344
1.934	3.936	17.889	1.326
2.715	3.252	18.083	1.341

The drawing of the part with the final optimized dimensions is depicted in Fig 4.1. If these results are compared with the previous ones, it can be seen that; when the failure criterion is not included, the minimum cost case was tending to be around the lower boundary of the die land constraint, which was 15. According to the derivations in structural analysis part, the failure criterion formulation is only dependent to the die land 'LO' among the optimization parameters. When the calculations are done according to the yield strength values of the material used, it can be seen that value of the die land lower than approximately 17.8 lead to failure under the working conditions. As it can be seen from the results, die land tended to take small and smaller values and approached to its minimum with the value of 17.889.

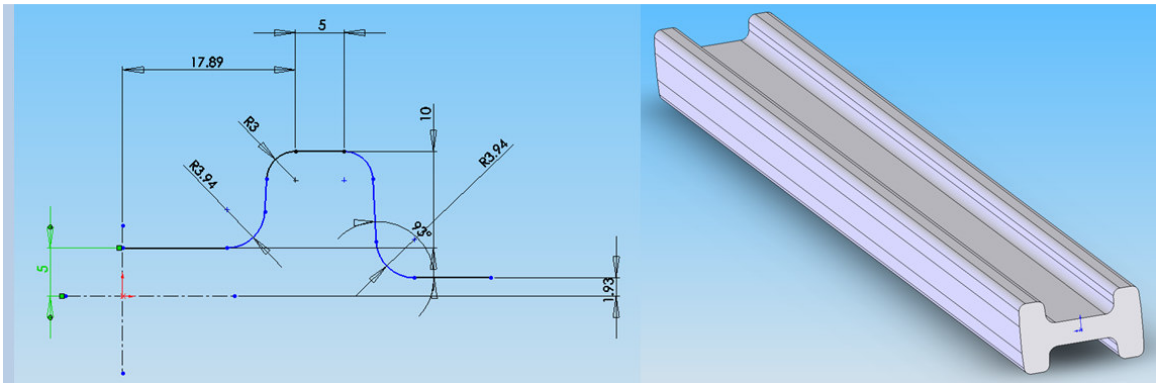

Figure 4.1 Final optimized shape of the profile

5. SUMMARY AND CONCLUSIONS

In this thesis, a concurrent design optimization methodology was proposed to minimize the cost of a cold forging process including material cost and post manufacturing operations.

The literature survey showed that although there are many examples about cost optimization of forging processes, there is only one paper about the optimization of forging with a concurrent approach which is a very general paper about the issue. This gap in the literature is the major motivation behind this thesis.

The analysis of the cold forging process is conducted by using ANSYS. An objective function is defined for the optimization based on three terms; material cost, manufacturing cost and post manufacturing (shearing) cost of the product. In order to quantify these terms part volume is used as a measure of material cost, strain energy of forging is used as a measure of the manufacturing cost and shear energy is used as a measure of post manufacturing cost.

The constraints of the problem that define the penalty functions are the physical constraints on the range of values for the optimization variables and the failure of the part under the predefined working conditions. The failure of the part is checked by calculating the maximum stress analytically and checking the failure criterion by taking the cold work hardening of the material into account.

Nelder-Mead is selected as the search algorithm since it is a robust zero-order algorithm which makes decisions based on the values of the objective function and does not require the calculation of any derivatives. An optimization code was developed using ANSYS Parametric Design Language incorporating the finite element model and the optimization procedure.

The part to be optimized is an I-beam which is under centric 22000N load in a simply supported configuration. Optimization variables chosen are the die land, L0, rib radiuses R1

and R3, which are equal to each other and burr thickness, BT. The optimized values of the variables for minimum cost are found to be 1,934 mm for burr thickness, 3,936 mm for the radiuses and 17,889 mm for die-land.

In addition to the optimized results for the given conditions, different cases are also considered and some general conclusions that can be used as a design guide for similar applications are drawn. The most effective parameter on the overall cost is found to be the die–land, L0, after some comparison is made between the results of two variable optimization cases. Besides, the most dominant term among the three cost terms that comprise the overall cost is found to be the material cost. As a final design guideline, the die land, L0 should be kept as short as possible. Although, this will increase the manufacturing cost, the overall cost was observed to be minimized with the decrease in the material cost by decreased L0.

The methodology proposed in this thesis is applicable to different types of materials and different cold forming processes. The three requirements to adapt the methodology proposed in this thesis to other cases are to obtain the material property data to choose a suitable set of optimization variables and to develop a reliable FE model of the process in concern. In addition to different geometric optimization variables, different process variables and constraints may be defined to enlarge the scope of the proposed method.

APPENDIX A: FLOW CURVE DATA USED IN MISO MODEL

Table A.1. Flow curve Data used in MISO Model

K		**n**	**ST 37**		
773		0.171			
Nr	**ε**	**σ**	**Nr**	**ε**	**σ**
1	0	0	**20**	0.500	686.6
2	0.001	244.1	**21**	0.550	697.9
3	0.002	267.1	**22**	0.600	708.3
4	0.003	286.3	**23**	0.700	727.3
5	0.004	300.7	**24**	0.800	744.1
6	0.005	312.4	**25**	0.900	759.2
7	0.025	411.4	**26**	1.000	773.0
8	0.060	477.8	**27**	1.250	803.1
9	0.100	521.4	**28**	1.500	828.5
10	0.150	558.8	**29**	1.750	850.6
11	0.200	587.0	**30**	2.000	870.3
12	0.250	609.9	**31**	2.250	888.0
13	0.275	619.9	**32**	2.500	904.1
14	0.300	629.2	**33**	2.750	919.0
15	0.325	637.8	**34**	3.000	932.8
16	0.350	646.0	**35**	3.250	945.6
17	0.375	653.6	**36**	3.500	957.7
18	0.400	660.9	**37**	3.750	969.0
19	0.450	674.3	**38**	4.000	979.8

APPENDIX B: THE NELDER - MEAD METHOD

The Nelder Mead Method is a robust zero order search algorithm not requiring numerical derivatives of the objective function. The method uses a simplex, which is a polytope of *n*+1vertices in *n* dimensions. For one variable, the simplex is a line segment. For two variables, the simplex is a triangle, and it becomes a tetrahedron (Figure B.1) for cases with three optimization variables.

Figure B.1. The simplex as a tetrahedron for three variables

Basically, the method is a pattern search that compares function values at vertices. The worst vertex, where the function value becomes largest, is rejected and replaced with a new vertex. A new simplex is formed and the search is continued. The process generates a sequence of simplex for which the function values at the vertices get smaller and smaller. Finally, the size of the simplex is reduced and the coordinates of the minimum point are found (Figure B.2).

The Nelder - Mead Algorithm is easier to explain for cases with two optimization variables, where the simplex is a triangle in 2D. Below is given the logical decisions made in Nelder Algorithm and short explanations of used terms. In this study, the Nelder-Mead algorithm is applied for three optimization variables resulting in four vertices. The differences between the two and three variable cases are also given below which is rarely depicted in text books.

The method requires the calculation of the objective function at three initial vertices. Then, the vertices are ordered from the smallest to greatest and denoted as *B* (best), *G* (good) and *W* (worst), respectively. For three optimization variables, initial vertices are denoted as *B* (best), *G* (good), *V* (worse) and *W* (worst).

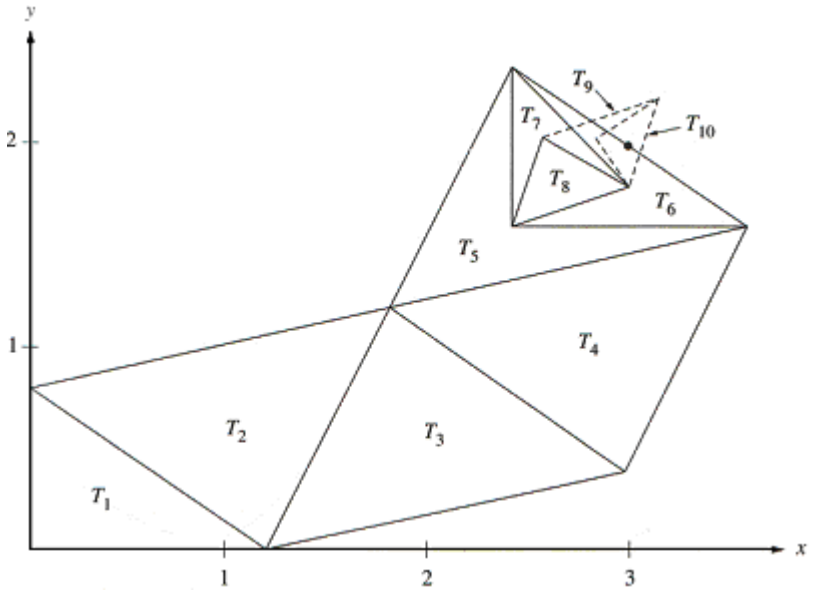

Figure B.2. The sequence of triangles converging to the minimum point [27]

The method requires the calculation of the objective function at three initial vertices. Then, the vertices are ordered from the smallest to greatest and denoted as *B* (best), *G* (good) and *W* (worst), respectively. For three optimization variables, initial vertices are denoted as *B* (best), *G* (good), *V* (worse) and *W* (worst).

The midpoint *M* is the point in the middle of line segment joining *B* and *G* vertices of triangle and calculated by Eq. B.1.

$$\vec{M} = \vec{B} + \vec{G} = \left(\frac{x_M + x_G}{2}, \frac{y_M + y_G}{2} \right) \tag{B.1}$$

For tetrahedron the midpoint M is found by Eq. B.2.

$$\vec{M} = \vec{B} + \vec{G} + \vec{V} = \left(\frac{x_M + x_G + x_V}{3}, \frac{y_M + y_G + y_V}{3}, \frac{z_M + z_G + z_V}{3} \right) \tag{B.2}$$

It is likely that the function takes smaller values away from W on the opposite side of the line AB. The behavior of the function on this side is checked on the reflection point R, which is obtained using Eq. B.3. Midpoint M and reflection point R are shown in Figure B.3 for triangular simplex and in Figure B.4 for tetrahedronal simplex.

$$\vec{R} = M + \left(\vec{M} - \vec{W} \right) \tag{B.3}$$

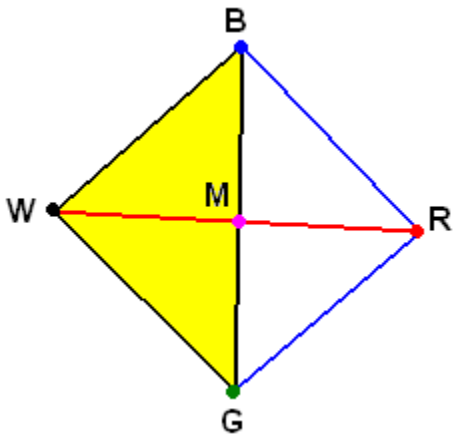

Figure B.3. Midpoint and reflection point for triangle

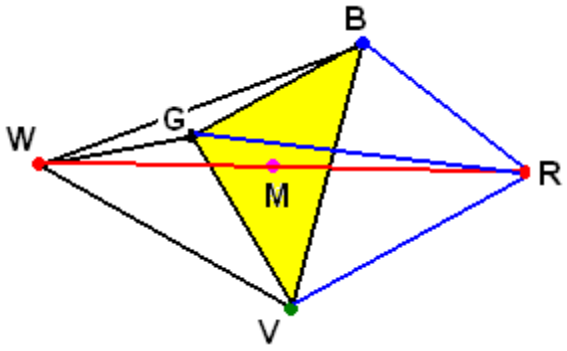

Figure B.4. Midpoint and reflection point for tetrahedron

If the reflection point yields a smaller function value, then it is extended to find a possibly better point lying further than the point *R*. Thus, the expansion point *E* is calculated (Eq. B.4). If *E* is a better point than *B*, then *W* is replaced by *R*, otherwise *W* is replaced by *R*. The equation giving expansion point is the same for triangular and tetrahedron simplex. Figure B.5 and Figure B.6 describe expansion of the simplex.

$$E = \vec{R} + \left(\vec{R} - \vec{M}\right) \tag{B.4}$$

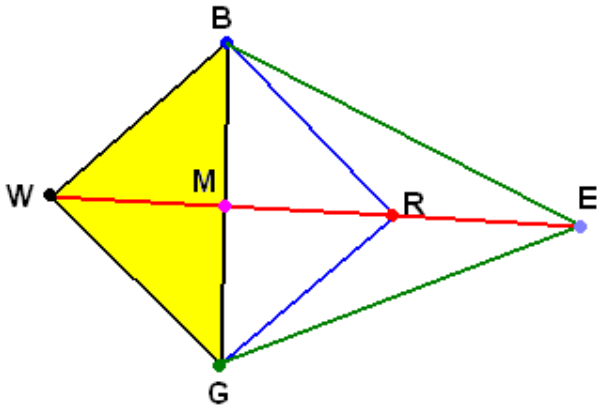

Figure B.5. Expansion using *R* in 2D

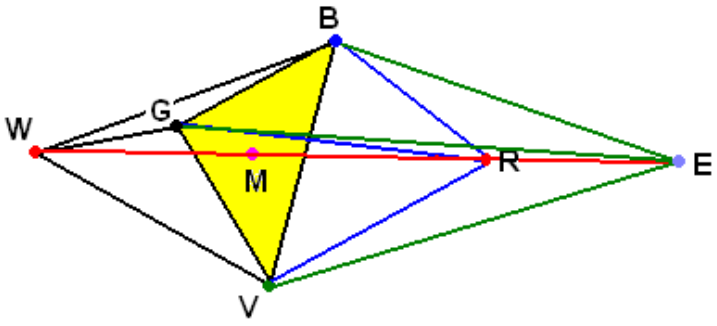

Figure B.6. Expansion using *R* in 3D

$$\vec{C} = \frac{\vec{W} + \vec{M}}{2} \tag{B.5}$$

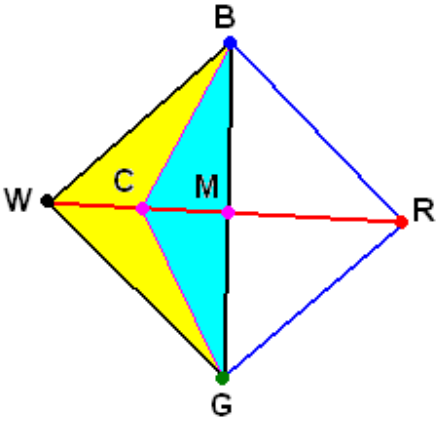

Figure B.7. New contracted triangle *BCG*

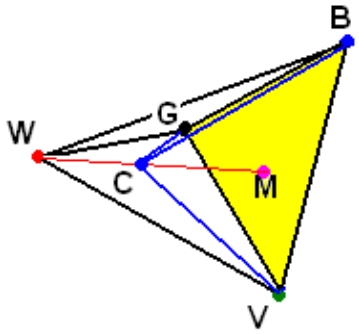

Figure B.8. Contraction of tetrahedron by *C*

If the objective function having a greater value at *C* compared to *W,* the triangle should be shrunk toward *B*. The resulting triangle is *BSM*. S is calculated by Eq. B.6. For tetrahedron, three shrink points are required, which are obtained by Eq. B.7, Eq. B.8 and Eq. B.9.

$$\vec{S} = \frac{\vec{B} + \vec{W}}{2} \tag{B.6}$$

$$\vec{S}_1 = \frac{\vec{B} + \vec{G}}{2} \tag{B.7}$$

$$\vec{S}_2 = \frac{\vec{B} + \vec{V}}{2} \tag{B.8}$$

$$\vec{S}_3 = \frac{\vec{B} + \vec{W}}{2} \tag{B.9}$$

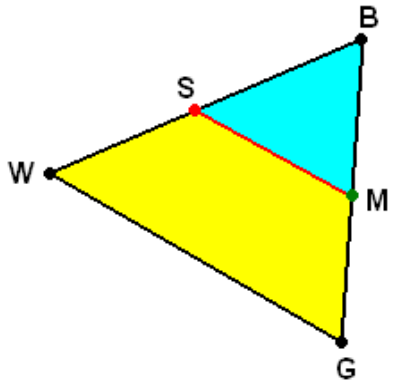

Figure B.9. Shrink toward *B*

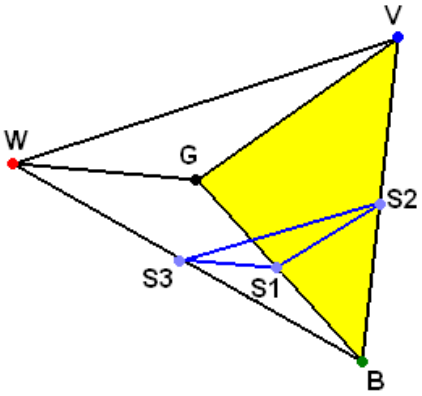

Figure B.10. Shrinking tetrahedron by S1, S2 and S2

Shrinkage of triangle and tetrahedron toward B are shown in Figure B. 9 and Figure B.10.

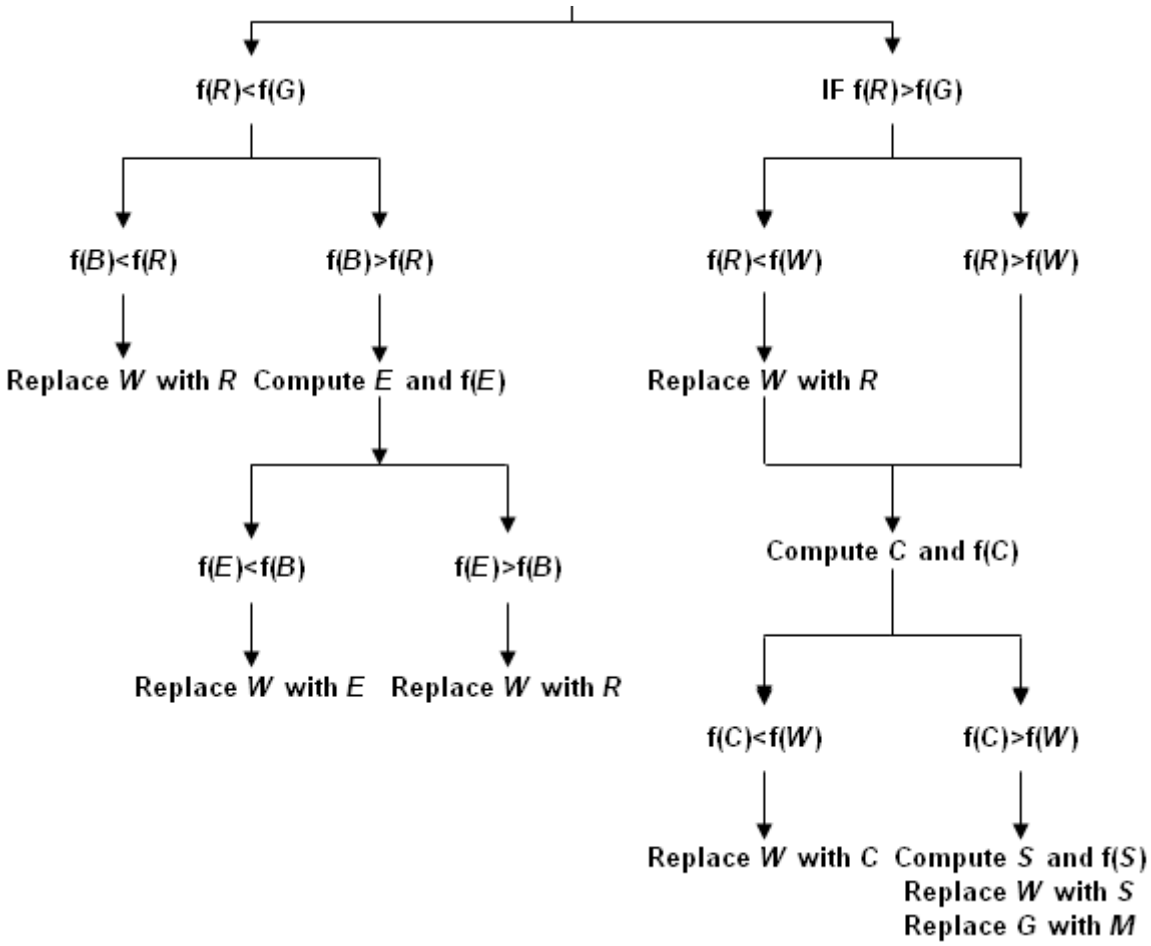

Figure B.11. Logical decisions for the Nelder-Mead algorithm

Process steps of the Nelder-Mead algorithm are given in Figure B.11. Following these steps and using equations given above, optimum points are obtained. Note that the Nelder-Mead algorithm gives the local minimum. In order to obtain the global minimum, optimization procedure needs to be repeated with different initial vertices

REFERENCES

1. Altan, T., Ngaile, Shen, G., 2005. Cold and Hot Forging- Fundamentals and Applications, ASM International, U.S.A., viii.

2. Gonzales, F. U., 2004. "A discussion on Modern Design Optimization Tools: Full Associativity of CAD, FEA and Event Simulators", ALGOR Inc., U.S.A

3. Chung, J. S., Hwang, S. M., 2002. Process Optimal Design in Forging by Genetic Algorithm, Journal of Manufacturing Science and Engineering, 124, 397-408.

4. Fourment, L., Chenot, J. L., 1996. Optimal design for non-steady-state metal forming processes - I: Shape optimization method, International Journal for Numerical Methods in Engineering, 39, 33–50.

5. Sönmez, F.Ö., Demir, A., 2007. Analytical Relations between Hardness and Strain for Cold Formed Parts, Journal of Materials Processing Technology, 186, 163-173.

6. Ou, H., Lan, J., Armstrong, C.G., Price, M.A., 2004. An FE simulation and optimization approach for the forging of aeroengine components, Journal of Materials Processing Technology, 151, 1-3, 208-216.

7. Gao, Z., Grandhi, R. V., 2000. Microstructure optimization in design of forging processes, International Journal of Machine Tools and Manufacture, 40, 5, 691-711.

8. Fourment, L., Balan, T., Chenot, J. L., 1996. Optimal design for non-steady-state metal forming processes - II: Application of shape optimization in forging, International Journal for Numerical Methods in Engineering, 39, 1, 51-65.

9. Shim, H., 2003. Optimal perform design for the free forging of 3D shapes by the sensitivity method, Journal of Materials Processing Technology, 134, 1, 99-107.

10. Park, J. J., Rebelo, N., Kobayashi, S., 1983. A new approach to preform design in metal forming with the finite element method, International Journal of Tool Design Research, 23, 71-79.

11. Kang, B. S., Kobayashi, S., 1994. Process sequence design in cold forging to form a constant velocity joint housing, International Journal of Machine Tool Design Research, 24, 1133-1146.

12. Kusiak, J., Thompson, E. G., 1989. Optimization techniques for extrusion die shape design. In Mattiason, K., Samuelson, A., Wood, R. D., Zienkiewicz, O. C. (eds.), Numerical Method in Industrial Forming Processes, 569-574, Boston.

13. Kusiak, J., 1990. Some aspects of optimization of metal forming tool shape design, Metalurgia 1 Odlewnicto, 16, 339-346.

14. Esche, S. K., Chassapis, C., Manoochehri, S., 2001. Concurrent product and process design in hot forging, Concurrent Engineering: Research and Applications, 9, 48-54.

15. Khoury, I., Giraud-Moreau, L., Lafon, P., Labergere, C., 2006. Towards an optimization of forging processes using geometric parameters, Journal of Materials Processing Technology, 177, 1-3, 224-227.

16. Schey, John A., 1999. Introduction to Manufacturing Processes, Third Edition, McGraw-Hill Science/Engineering/Math, U.S.A.

17. http://www.matweb.com/search/DataSheet.aspx?MatID=14015. (Accessed September 2008)

18. http://www.bdtradeinfo.com/members/search_des.asp?ID=10988. (Accessed September 2008)

19. Tumer, H., 2006. Optimum Preform And Die Shape Design For Improved Hardness Distribution In Cold Forged Parts, M.S. Thesis, Bogazici University

20. Megson, T. H. G., 2000. Structural and Stress Analysis, Butterworth-Heinemann, Germany.

21. Ansys, Release 10.0 Documentation, 2005. ANSYS Inc., U.S.A

22. Gouveia, B.P.P.A., Rodrigues, J.M.C., Bay, N., Martins, P. A. F., 1999. Finite Element Modeling of Cold Forward Extrusion, Journal of Materials Processing Technology, 94, 85-93.

23. Hur, K. D., Choi, Y., Yeo, H. T., 2003. A Design Method for Cold Forward Extrusion using FE Analysis, Finite Elements in Analysis and Design, 40, 173-185.

24. Petruska, J., Janicek, L., 2003. On the Evaluation of Strain Inhomogeneity by Hardness Measurement of Formed Products, Journal of Materials Processing Technology, 143-144, 300-305.

25. Roy, S., Ghosh, S., Shivpuri, R., 1997. A new Approach to Optimal Design of Multi-Stage Metal Forming Processes with Micro Genetic Algorithms, International Journal of Machine Tools and Manufacture, 37, 1, 29-44.

26. Mathews, H., Fink, K. D., 1999. Numerical Methods Using Matlab, Third Edition, Prentice Hall Inc., New Jersey.